Hindawi
Advances in Condensed Matter Physics
Volume 2021, Article ID 8110754, 10 pages
https://doi.org/10.1155/2021/8110754

Research Article

Impurity Substitution Enhances Thermoelectric Figure of Merit in Zigzag Graphene Nanoribbons

Saeideh Ramezani Akbarabadi[1] **and Mojtaba Madadi Asl**[2]

[1]*Department of Physics, University of Guilan, Rasht, Iran*
[2]*Department of Physics, Institute for Advanced Studies in Basic Sciences (IASBS), Zanjan, Iran*

Correspondence should be addressed to Mojtaba Madadi Asl; mojtabamadadi7@gmail.com

Received 14 July 2021; Accepted 19 October 2021; Published 31 October 2021

Academic Editor: Charles Rosenblatt

The thermoelectric properties of zigzag graphene nanoribbons (ZGNRs) are sensitive to chemical modification. In this study, we employed density functional theory (DFT) combined with the nonequilibrium green's function (NEGF) formalism to investigate the thermoelectric properties of a ZGNR system by impurity substitution of single and double nitrogen (N) atoms into the edge of the nanoribbon. N-doping changes the electronic transmission probability near the Fermi energy and suppresses the phononic transmission. This results in a modified electrical conductance, thermal conductance, and thermopower. Ultimately, simultaneous increase of the thermopower and suppression of the electron and phonon contributions to the thermal conductance leads to the significant enhancement of the figure of merit in the perturbed (i.e., doped) system compared to the unperturbed (i.e., nondoped) system. Increasing the number of dopants not only changes the nature of transport and the sign of thermopower but also further suppresses the electron and phonon contributions to the thermal conductance, resulting in an enhanced thermoelectric figure of merit. Our results may be relevant for the development of ZGNR devices with enhanced thermoelectric efficiency.

1. Introduction

Low-dimensional thermoelectric devices can be potentially utilized for a wide range of applications, e.g., in cooling, heating, and energy harvesting systems [1, 2]. However, limited efficiency of thermoelectric systems critically restricts the practical use of the thermoelectric effect at the nanoscale. The efficiency of a thermoelectric system can be expressed by the figure of merit, i.e., $ZT = S^2TG/K$. The figure of merit is shaped by the interplay between the thermopower or Seebeck coefficient (S), electrical conductance (G), thermal conductance (K), and temperature (T). Hence, increasing the electrical conductance and thermopower or restriction of the thermal conductance can enhance the thermoelectric figure of merit [3, 4]. Such a strategy is challenging in practice due to the interdependence of the thermoelectric coefficients.

Novel or engineered materials provide an unprecedented opportunity to overcome this challenge by offering favorably manipulated physical and chemical properties to attain enhanced thermoelectric efficiency [3–8]. Due to its unique electronic structure and physical properties [9, 10], graphene is one of the interesting low-dimensional materials that consists of a monolayer of carbon atoms organized in a hexagonal lattice. Experimental studies have shown that the realization of graphene nanoribbons (GNRs) with controlled edge orientation is conceivable, e.g., by scanning tunneling microscope (STM) lithography techniques [11]. In particular, zigzag graphene nanoribbons (ZGNRs) can be regarded as a suitable candidate for thermoelectric effect studies due to their

metallic nature and high electrical/thermal conductivity at room temperature [10, 12, 13]. By using different methods, several experiments measured charge transport and thermoelectric properties in graphene-based systems [14, 15].

In general, several factors such as changing the contact geometry or length of the structure can modify the electronic and transport properties of low-dimensional devices at the level of molecules [16–19]. The ZGNRs are no exception. In this context, doping by chemical impurity, e.g., boron (B) atoms or nitrogen (N) atoms, is one of the modifications that can significantly change the electronic and transport properties of ZGNRs [20–22], supported by experimental observations [23, 24]. For instance, doping concentration or dopant position can modify the electronic structure of ZGNRs, such that both semiconducting and half-metallic behaviors can be achieved when the system is subjected to external electrical field [25]. BN codoping of ZGNRs can result in the emergence of bound and quasi-bound states leading to modified transport properties [20]. Therefore, chemical doping of ZGNRs seems to be a desirable method to manipulate the charge carrier transport in ZGNRs [26].

By the same token, thermoelectric properties of graphene-based systems are prone to physical or chemical perturbations [6, 27], especially to impurity doping [4, 5, 28]. For instance, the sign of thermopower is typically determined by the charge transport polarization of the system due to the charge donating/accepting nature of dopants [4]. Motivated by experimental findings, theoretical studies explored various aspects of thermoelectric properties in graphene-based systems [7, 29–31]. It has been shown that the figure of merit can be significantly enhanced by periodically embedding hexagonal BN atoms into hybrid GNRs due to the simultaneous increase of thermopower and suppression of the thermal conductance [5]. Furthermore, it has been argued that the thermoelectric figure of merit of organic molecular junctions with ZGNR electrodes can be enhanced by N-doping due to the suppression of phonon contribution to the thermal conductance [4]. The origin of such modulations can be traced back to the doping-induced modification of energy separation between the highest occupied molecular orbital (HOMO) and the lowest unoccupied molecular orbital (LUMO), i.e., the HOMO – LUMO gap, in the transmission spectrum [4].

In this study, we employed density functional theory (DFT) combined with the nonequilibrium green's function (NEGF) formalism in the linear response regime to investigate the thermoelectric properties of a ZGNR-based system by the impurity doping of single and double N atoms into the edge of the nanoribbon. We first assumed an unperturbed (i.e., nondoped) system and inspected the electrical conductance, thermal conductance, thermopower, and figure of merit. We then perturbed (i.e., doped) the system with the substitution of edge carbon atoms with a single N atom or double N atoms and repeated our calculations. A comparison between the results obtained for the unperturbed system with those obtained from the perturbed system showed that the electrical conductance, electron and phonon contributions to the thermal conductance and thermopower are notably modified in the doped system resulting in an enhanced thermoelectric figure of merit.

In particular, our results show that when the ZGNR is perturbed with impurity, the electronic transmission probability near the Fermi energy is notably modified and the phononic transmission is suppressed for a wide range of energies in comparison to the unperturbed system. Substitution of the impurity decreased the electrical conductance of the perturbed ZGNR; however, the thermopower was significantly enhanced, and both the electron and phonon contributions to the thermal conductance were simultaneously suppressed. This ultimately led to the enhancement of the thermoelectric figure of merit in the perturbed ZGNR compared to the unperturbed one. In addition, increasing the number of edge-doped N atoms (from a single atom to double atoms) favorably tuned the thermoelectric properties of the ZGNR-based system (i.e., both the electron and phonon contributions to the thermal conductance were suppressed), leading to an enhanced figure of merit in the perturbed system.

2. Materials and Methods

The unperturbed hydrogen-passivated ZGNR system is schematically shown in Figure 1(a) that is characterized with the central scattering region (labeled center) with width $w =$ 8 atoms connected to semiinfinite metallic ZGNRs (labeled left/right). To construct the perturbed (i.e., doped) structures, edge carbon atoms of ZGNR were substituted by a single N atom (Figure 1(b)) or double N atoms (Figure 1(c)). DFT calculations were performed as implemented in the SIESTA computer program [32], within the generalized gradient approximation (GGA) of Perdew–Burke–Ernzerhof (PBE) [33]. The transport properties of the structure were calculated by the NEGF formalism implemented in the TranSIESTA routine [34]. The Brillouin zone sampling was performed using $1 \times 1 \times 100$ k-point sampling. The energy cutoff was 150 Ry.

The electron transmission spectrum of the system was calculated using the Landauer–Büttiker formalism given in terms of the green's function [35]:

$$T_{el}(\varepsilon) = Tr\left[\mathbf{G}^{r}(\varepsilon)\Gamma_{L}(\varepsilon)\mathbf{G}^{a}(\varepsilon)\Gamma_{R}(\varepsilon)\right], \quad (1)$$

where $\Gamma_{L/R} = -2\mathrm{Im}\Sigma_{L/R}$ can be expressed by the self-energy $\Sigma_{L/R}$ of the left (L) or right (R) lead, $\mathbf{G}^{r}(\varepsilon) = [\varepsilon\mathbf{S} - \mathbf{H} - \Sigma_{L}(\varepsilon) - \Sigma_{R}(\varepsilon)]^{-1}$ denotes the retarded green's function, and the advanced green's function can be calculated via the relation $\mathbf{G}^{a}(\varepsilon) = [\mathbf{G}^{r}(\varepsilon)]^{\dagger}$, where $\mathbf{H}$ and $\mathbf{S}$ are the Hamiltonian matrix and the overlap matrix, respectively.

Charge current (I) and heat current (I_Q) were calculated based on the Keldysh NEGF formalism [36]. In the linear response regime, the temperature gradient (ΔT) and voltage difference (ΔV) are small; hence, charge current and heat current can be approximated (to the first order) in terms of ΔT and ΔV and [35, 36]

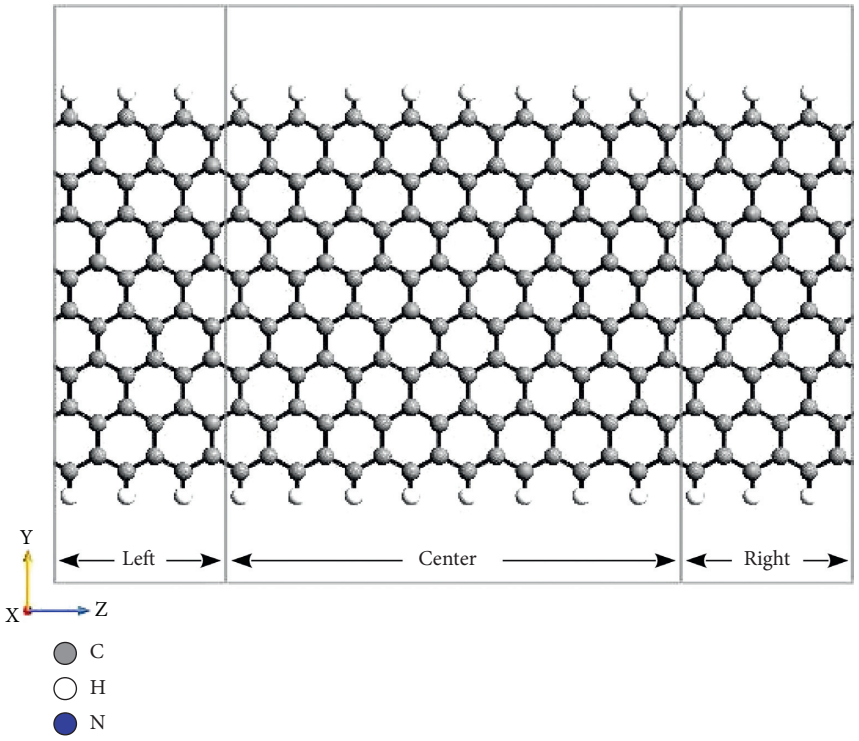

(a)

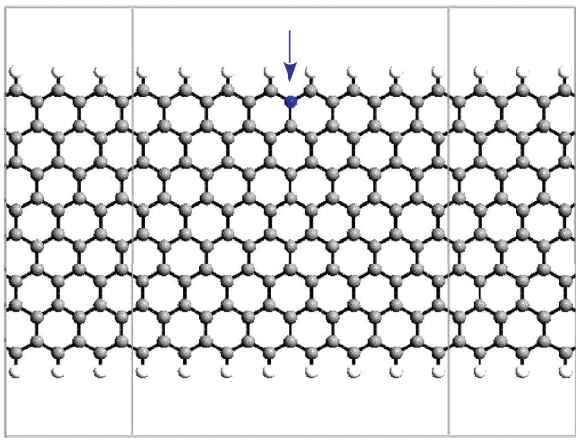

(b)

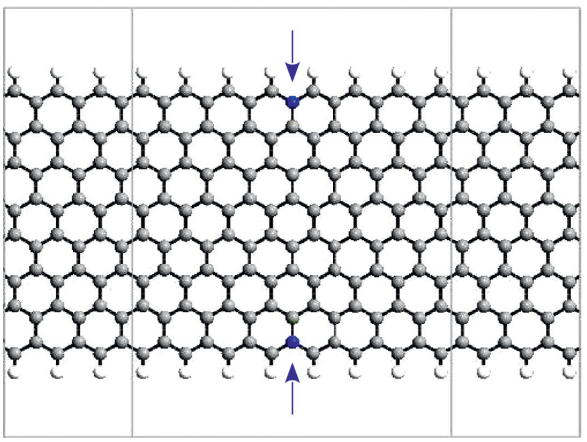

(c)

Figure 1: Schematic representation of the ZGNR system. The central region (labeled center) with width $w = 8$ atoms is connected to semiinfinite ZGNRs (labeled left/right). (a) The unperturbed ZGNR. (b) The ZGNR perturbed with a single N atom (denoted by arrow). (c) The ZGNR perturbed with double N atoms (denoted by arrows).

$$I = e^2 L_0 \Delta V + \frac{e}{T} L_1 \Delta T,$$
$$I_Q = -eL_1 \Delta V - \frac{1}{T} L_2 \Delta T, \tag{2}$$

where $L_n = \hbar^{-1} \int d\varepsilon (\varepsilon - \mu)^n T(\varepsilon)(-\partial f(\varepsilon)/\partial \varepsilon)$ is the Lorenz function, μ represents the chemical potential, and $f(\varepsilon)$ is the equilibrium Fermi–Dirac function.

The thermoelectric coefficients can be expressed in terms of the quantities L_n. The electrical conductance, the electron contribution to the thermal conductance, and the thermopower can be calculated as follows, respectively:

$$G = e^2 L_0, \tag{3}$$

$$K_{el} = \left(\frac{1}{T}\right)\left(\frac{L_2 - L_1^2}{L_0}\right), \tag{4}$$

$$S = -\frac{\Delta V}{\Delta T}|_{I=0} = -\left(\frac{1}{eT}\right)\left(\frac{L_1}{L_0}\right). \tag{5}$$

The interplay between thermoelectric coefficients ultimately determines the figure of merit of the system as follows:

$$ZT = S^2 TG/\left(K_{el} + K_{ph}\right), \tag{6}$$

where both the electronic thermal conductance (K_{el}) and phononic thermal conductance (K_{ph}) are considered in this study to provide a more accurate estimation of the figure of merit.

By using the classical methods, the phonon contribution to thermal conductance can be calculated from the phonon transmission function ($T_{ph}(\omega)$) via the Landauer-type formula [37]:

$$K_{ph} = \frac{\hbar^2}{2\pi} \int_0^\infty d\omega T_{ph}(\omega)\left(\frac{\partial f_{ph}(\omega)}{\partial \omega}\right), \tag{7}$$

where $f_{ph}(\omega)$ represents the Bose–Einstein distribution function. Phonons can be described by the classical dynamical matrix of the system. The ReaxFF potential was used for the parameterization of the potential. In the elastic transport regime, the phonon transmission function and the frequency of phonons (ω) can be expressed in terms of NEGF:

$$T_{ph}(\omega) = Tr\left[\Lambda_R(\omega)\mathbf{D}(\omega)\Lambda_L(\omega)\mathbf{D}^\dagger(\omega)\right]. \tag{8}$$

Then, the phonon-retarded green's function was calculated accordingly by substituting $\mathbf{H} \longrightarrow \mathbf{K}$, $\varepsilon\mathbf{S} \longrightarrow \omega^2\mathbf{M}$, and $\Sigma_{L/R} \longrightarrow \Pi_{L/R}$:

$$\mathbf{D}(\omega) = \left[\omega^2\mathbf{M} - \mathbf{K} - \Pi_L(\omega) - \Pi_R(\omega)\right]^{-1}, \tag{9}$$

where $\mathbf{K}$ is the force constant matrix, $\mathbf{M}$ denotes a diagonal matrix comprising the atomic masses, $\Pi_{L/R}$ is the self-energy of the left (L) or right (R) lead, and $\Lambda_{L/R}(\omega) = i[\Pi_{L/R}(\omega) - \Pi_{L/R}^\dagger(\omega)]$.

3. Results and Discussion

3.1. The Effect of Impurity Substitution on Transmission Spectrum. The edge atoms of ZGNR were hydrogen-passivated to attain more stable physical properties and to saturate the carbon $2p$ edge states that can lead to the emergence of localized states in the pure system [38]. We first considered the unperturbed (i.e., nondoped) ZGNR system shown in Figure 1(a) and calculated the electronic and phononic transmission spectra as a function of energy. As shown in Figure 2(a) (green curve), the electronic transmission spectrum of the unperturbed ZGNR system exhibits a peak at the Fermi energy (inset of Figure 2(a), green curve). Then, the ZGNR system was perturbed (i.e., doped), so that edge carbon atoms were substituted with a single N atom (N-ZGNR), as shown in Figure 1(b), or with double N atoms (NN-ZGNR), as shown in Figure 1(c). The corresponding electronic transmission spectrum of the perturbed systems is shown in Figure 2(a). In both N-ZGNR (blue curve) and NN-ZGNR (red curve), the transmission probability is relatively suppressed near the Fermi energy in comparison to the unperturbed ZGNR system (green curve).

Furthermore, the inset to Figure 2(a) shows that impurity substitution leads to the emergence of new resonance peaks around the Fermi energy and, in this way, may dramatically change the nature of the charge transport in the system, i.e., HOMO-dominated (p-type) transport vs. LUMO-dominated (n-type) transport, due to the electron-accepting nature of N-doping [4]. Interestingly, the N-ZGNR system shows a HOMO-dominated transport since the HOMO peak is located closer to the Fermi energy than the LUMO peak (inset of Figure 2(a), blue curve). However, transport in the NN-ZGNR system occurs through LUMO which is closer to the Fermi energy than HOMO (inset of Figure 2(a), red curve). This suggests that the number of N atoms used for doping may crucially determine the nature of transport in the system.

The phonon-contributed transmission spectrum of the considered ZGNR systems is superimposed, as shown in Figure 2(b). The comparison of the phononic transmission between the unperturbed (ZGNR) and perturbed (N-ZGNR and NN-ZGNR) systems clearly shows that N-doping can suppress the phononic transmission for a wide range of energies. In particular, increasing the number of dopants (from a single N atom to double N atoms) further suppressed the phononic transmission, implying that impurity substitution may be a suitable method to restrict phonon contribution to the transmission leading to an enhanced thermoelectric figure of merit.

3.2. The Effect of Impurity Substitution on Thermoelectric Properties. The temperature dependency of thermoelectric properties of the unperturbed (ZGNR) and perturbed (N-ZGNR and NN-ZGNR) systems is shown in Figure 3. The electrical conductance of the ZGNR (green curve) and N-ZGNR (blue curve) systems is decreased with temperature, whereas the electrical conductance of the NN-ZGNR (red curve) system is relatively increased (Figure 3(a)). The

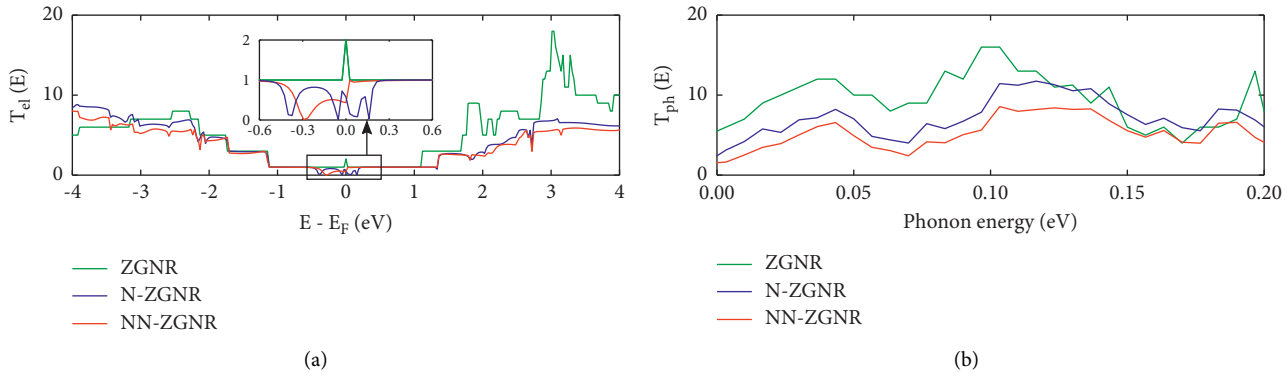

Figure 2: Electronic transmission spectrum (a) and phononic transmission spectrum (b) shown for the unperturbed ZGNR (green), N-ZGNR (blue), and NN-ZGNR (red) systems as a function of energy evaluated at $T = 300$ K.

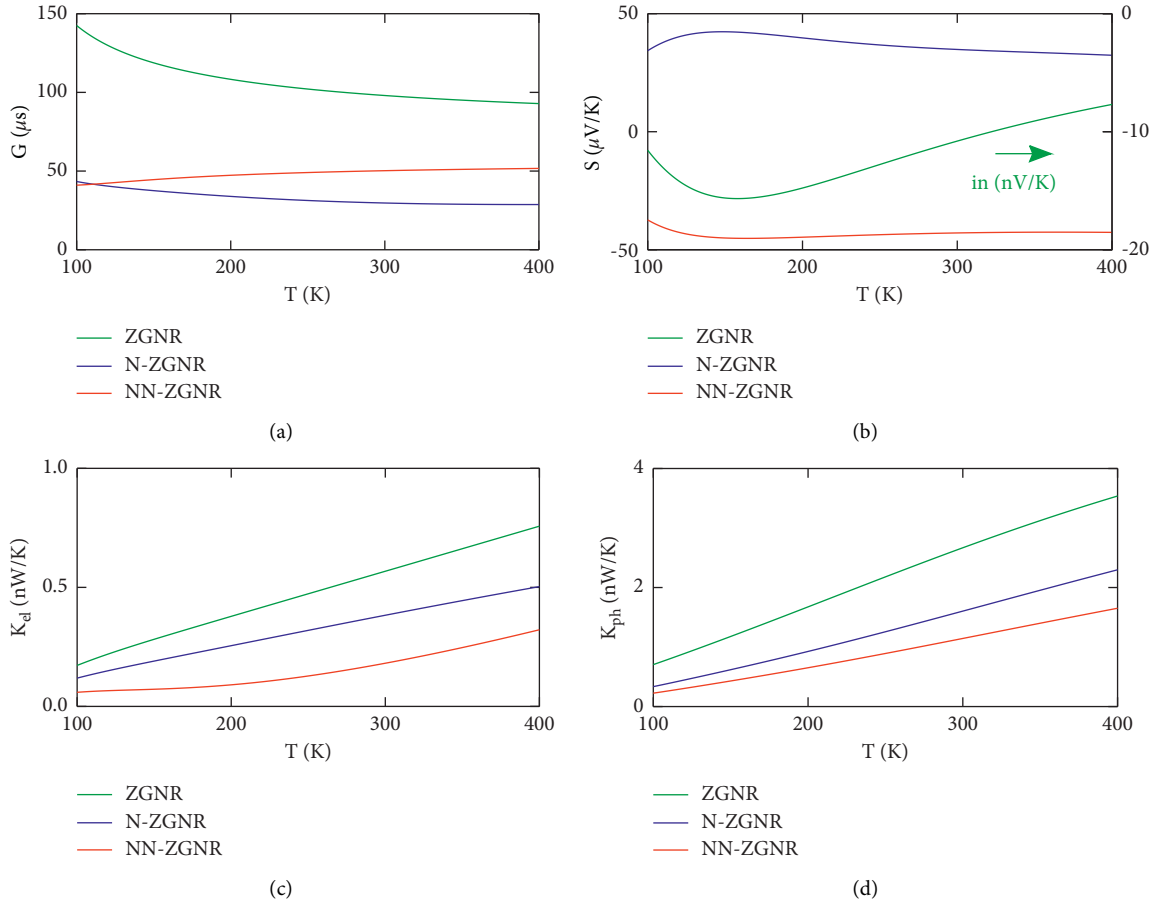

Figure 3: Temperature dependency of electrical conductance (a), thermopower (b), electron contribution to the thermal conductance (c), and phonon contribution to the thermal conductance (d) calculated for the ZGNR (green), N-ZGNR (blue), and NN-ZGNR (red) systems. The colored arrow in panel B indicates that the corresponding curve is depicted against the y2-axis (right).

origin of the ascending/descending trend of the electrical conductance can be traced back to the behavior of the Fermi derivative $(-\partial f/\partial\varepsilon)$ associated with the L_0 term in equation (3) with temperature. For example, as shown in Figure 4(a) for the ZGNR system, $T(\varepsilon)(-\partial f/\partial\varepsilon)$ gets broadened around the Fermi energy with increasing the temperature. This ultimately leads to the decrease of the electrical conductance with temperature. Same argument can be brought forward for the decreasing/increasing trend of electrical conductance in the N-ZGNR and NN-ZGNR systems.

In general, increasing the thermopower can significantly enhance the thermoelectric figure of merit since $ZT \propto S^2$. On the other hand, the sign of the thermopower reveals the nature of transport through the system [39, 40]. A positive

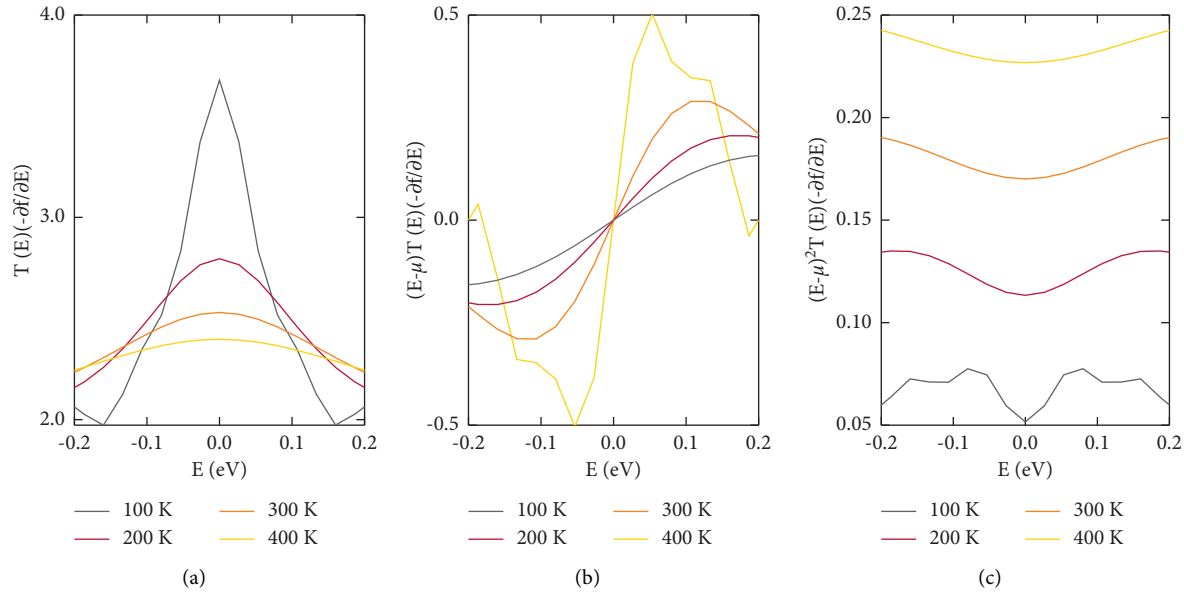

FIGURE 4: Temperature dependency of Lorenz functions is exemplary shown for the unperturbed ZGNR system. (a) $T(\varepsilon)(-\partial f/\partial\varepsilon)$. (b) $(\varepsilon-\mu)T(\varepsilon)(-\partial f/\partial\varepsilon)$. (c) $(\varepsilon-\mu)^2T(\varepsilon)(-\partial f/\partial\varepsilon)$.

thermopower is the indicator of p-type (HOMO-dominated) transport, whereas n-type (LUMO-dominated) transport is characterized with a negative thermopower. Here, the thermopower of the ZGNR (green curve) and NN-ZGNR (red curve) systems is negative, as shown in Figure 3(b). However, interestingly, the N-ZGNR system showed a positive thermopower suggesting that the number of N atoms used for impurity substitution may change the nature of transport in the system (Figure 3(b), blue curve).

Furthermore, the thermopower of the ZGNR (green curve) and NN-ZGNR (red curve) systems in Figure 3(b) first slightly decreases with temperature up to ~150 K and then relatively increases with temperature. On the contrary, the thermopower of N-ZGNR (blue curve) is increased till ~150 K and then decreased with temperature. These different temperature-dependent behaviors of the thermopower can be ascribed to $(\varepsilon-\mu)T(\varepsilon)(-\partial f/\partial\varepsilon)$ that determines the behavior of the thermopower by the L_1 term via equation (5). $(\varepsilon-\mu)T(\varepsilon)(-\partial f/\partial\varepsilon)$ is exemplary shown for the ZGNR system in Figure 4(b) that is increased near the Fermi energy when the temperature is increased. Similar reasoning can be used to explain the temperature dependency of thermopower in the case of N-ZGNR and NN-ZGNR systems.

The temperature dependency of thermal conductance is shown in Figures 3(c) and 3(d). Both the electron- and phonon-contributed thermal conductances of all considered systems (i.e., ZGNR, N-ZGNR, and NN-ZGNR) are increased with temperature. This was expected since electrons and holes carry more thermal energy when the temperature increases. Note that the behavior of the electron contribution to thermal conductance is mostly determined by equation (4) comprising $(\varepsilon-\mu)^2T(\varepsilon)(-\partial f/\partial\varepsilon)$ that is associated with the L_2 term [4]. $(\varepsilon-\mu)^2T(\varepsilon)(-\partial f/\partial\varepsilon)$ is exemplary shown for the ZGNR system, as shown in Figure 4(c). Clearly, increasing of the temperature has increased this term, so that ultimately the electron contribution to thermal conductance is enhanced. The same argument is true for the N-ZGNR and NN-ZGNR systems. The phonon contribution to thermal conductance determined by equation (7) also follows the same ascending trend.

In addition, both the electron and phonon contributions to the thermal conductance are suppressed when the system is perturbed with N impurity substitution (Figures 3(c) and 3(d) (green curve) and Figures 3(c) and 3(d) (blue/red curve)). It is interesting that increasing the number of N atoms used for the doping (from a single N atom in the N-ZGNR system to double N atoms in the NN-ZGNR system) further suppressed the electron and phonon contributions to the thermal conductance (Figures 3(c) and 3(d) (blue curve) and Figures 3(c) and 3(d) (red curve)). This can be beneficiary since according to equation (6), restriction of the thermal conductance can lead to the enhancement of the thermoelectric figure of merit.

The results obtained for the thermoelectric figure of merit are shown in Figure 5. To emphasize the role of phonon contribution in the reduction of the figure of merit, the electronic figure of merit is also drawn separately, as shown in Figure 5(a), that is, expectedly greater than the total figure of merit, as shown in Figure 5(b). Both the electronic and total figures of merit for the unperturbed ZGNR system are negligible. However, when the system is doped with N atoms, either single (N-ZGNR) or double (NN-ZGNR), both the electronic and total figures of merit are notably enhanced (Figure 5 (green curve) and Figure 5 (blue/red curve)).

The temperature dependency of the thermoelectric figure of merit can be traced back to the behavior of the electrical conductance, thermopower, and electron and

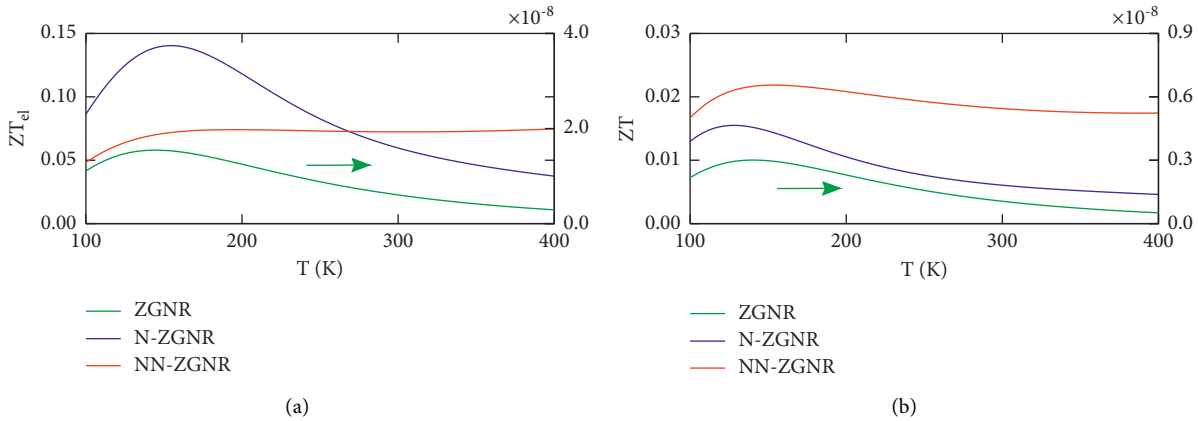

Figure 5: Temperature dependency of electron contribution to the figure of merit (a) and total figure of merit (b) calculated for the ZGNR (green), N-ZGNR (blue), and NN-ZGNR (red) systems. The colored arrows indicate that the corresponding curves are depicted against the y2-axis (right).

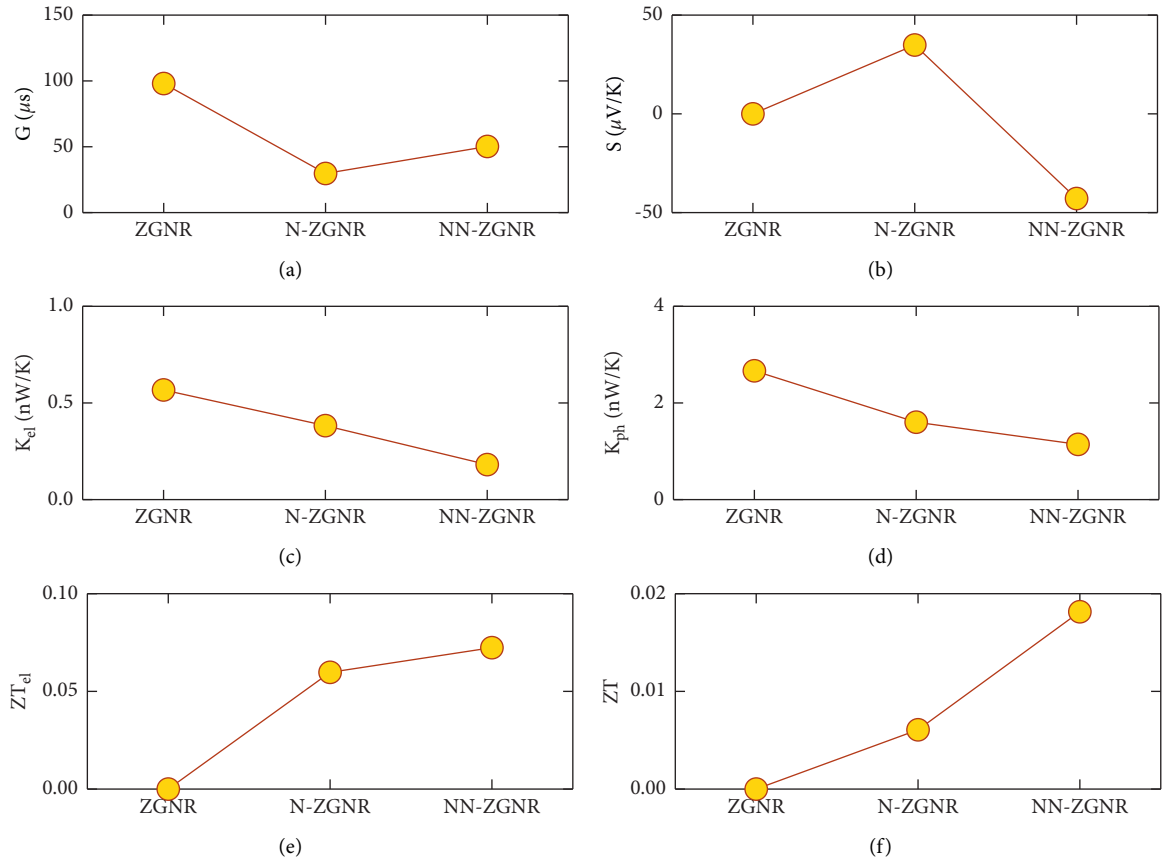

Figure 6: Comparative representation of thermoelectric coefficients for different configurations of the ZGNR system evaluated at $T = 300$ K. Electrical conductance (a), thermopower (b), electron contribution to the thermal conductance (c), phonon contribution to the thermal conductance (d), electronic figure of merit (e), and total figure of merit (f) calculated for the ZGNR, N-ZGNR, and NN-ZGNR systems.

phonon contributions to the thermal conductance, as shown in Figure 3. The interplay between these variables ultimately shapes the figure of merit of the system. Notably, the electronic figure of merit of the N-ZGNR system is first increased with temperature up to ~150 K, and then decreased, whereas the electronic figure of merit of the NN-ZGNR system is relatively robust to temperature changes (see Figure 5(a)). The N-ZGNR system exhibits the greatest value of the figure of merit among all considered configurations, i.e., ZT ≈ 0.15 at ~150 K.

3.3. Comparison between the Unperturbed and Perturbed Systems. To provide a representative estimation of the effect of impurity substitution on the electrical conductance, thermopower, thermal conductance, and figure of merit at room temperature, we compared the obtained results at $T = 300\,\mathrm{K}$, as shown in Figure 6. In general, the impurity substitution of N atoms decreased the electrical conductance of the ZGNR system irrespective of the number of N atoms used for doping (Figure 6(a)). However, this reduction was slightly greater in the N-ZGNR system than the NN-ZGNR system. The magnitude of thermopower was significantly enhanced by N-doping in comparison to the unperturbed ZGNR system (Figure 6(b)). Interestingly, the N-ZGNR system showed a positive value for the thermopower, whereas the thermopower of the NN-ZGNR system was negative.

Notably, both the electron contribution to the thermal conductance (Figure 6(c)) and the phonon contribution to the thermal conductance (Figure 6(d)) were decreased with N-doping. Interestingly, increasing the number of N atoms used for impurity substitution from ZGNR ($N = 0$) to N-ZGNR ($N = 1$) and NN-ZGNR ($N = 2$) further restricted the electron/phonon contribution to the thermal conductance. This is really promising, since the figure of merit can be significantly enhanced by the suppression of the thermal conductance.

Ultimately, both the electronic and total figures of merit were remarkably enhanced following impurity substitution of N atoms compared to the unperturbed system. As shown in Figure 6(e), the electronic figure of merit increased from 6.0×10^{-9} in ZGNR to 0.060 in N-ZGNR and then to 0.075 in NN-ZGNR (this was the greatest value obtained at room temperature). The value of the total figure of merit was, in general, smaller than the electronic figure of merit, since the phonon contribution to the thermal conductance was considered to provide a more accurate estimation (Figures 6(e) and 6(f)). In this case, the figure of merit increased from 1.0×10^{-9} in ZGNR to 0.007 in N-ZGNR and then to 0.020 in NN-ZGNR (Figure 6(f)).

4. Conclusions

In summary, we theoretically investigated the effect of N-doping on the thermoelectric properties of a ZGNR system. Our results show that the impurity substitution of N atoms into the ZGNR-based system can modify the electronic transmission probability near the Fermi energy. In addition, the phononic transmission is suppressed. In this way, the electrical conductance, thermopower, and thermal conductance of the system can be significantly regulated. In particular, the thermoelectric figure of merit that is determined by the interplay between these variables can be favorably tuned (enhanced). Here, this enhancement was achieved by the simultaneous suppression of the electron and phonon contributions to the thermal conductance and significant increase of the thermopower of the system.

Furthermore, another notable observation was that increasing the number of N atoms used for doping of the ZGNR system can be beneficiary. First, it can change the nature of transport, so that the N-ZGNR system showed a HOMO-dominated (p-type) transport, whereas the transport character of NN-ZGNR was LUMO-dominated (n-type). Second, the magnitude of the thermopower was relatively robust to the number of N atoms, but not its sign. The N-ZGNR system showed a positive thermopower, whereas the NN-ZGNR system showed a negative thermopower. Third, increasing the number of dopants resulted in further suppression of the electron and phonon contributions to the thermal conductance and ultimately led to the significant enhancement of the figure of merit in the perturbed ZGNR systems.

Ultimately, in this study, we utilized DFT combined with NEGF formalism to investigate the electronic and thermoelectric properties of a ZGNR system. However, a number of previous studies used a variety of transfer-matrix methods to calculate electronic properties of even larger nanoribbon systems than the ones studied here [41, 42]. In particular, previous approaches investigated various nanoribbon systems using transfer-matrix methods to understand the overall trend of electronic properties for large nanoribbons that would otherwise be hard to obtain with DFT and NEGF approaches [41, 42].

Data Availability

The data generated or analyzed during this study are included within this article.

Conflicts of Interest

The authors declare that they have no conflicts of interest.

Authors' Contributions

S. R. and M. M. conceived the study, analyzed the results, and reviewed the article, S. R. conducted the theoretical approximations and numerical simulations, and M. M. wrote the article.

References

[1] F. J. DiSalvo, "Thermoelectric cooling and power generation," *Science*, vol. 285, no. 5428, pp. 703–706, 1999.

[2] L. E. Bell, "Cooling, heating, generating power, and recovering waste heat with thermoelectric systems," *Science*, vol. 321, no. 5895, pp. 1457–1461, 2008.

[3] F. Mazzamuto, V. Hung Nguyen, Y. Apertet et al., "Enhanced thermoelectric properties in graphene nanoribbons by resonant tunneling of electrons," *Physical Review B*, vol. 83, no. 23, Article ID 235426, 2011.

[4] S. R. Akbarabadi, H. Rahimpour Soleimani, Z. Golsanamlou, and M. Bagheri Tagani, "Enhanced thermoelectric properties in anthracene molecular device with graphene electrodes: the role of phononic thermal conductance," *Scientific Reports*, vol. 10, pp. 1–13, Article ID 10922, 2020.

[5] K. Yang, Y. Chen, R. D'Agosta, Y. Xie, J. Zhong, and A. Rubio, "Enhanced thermoelectric properties in hybrid graphene/boron nitride nanoribbons," *Physical Review B*, vol. 86, no. 4, Article ID 045425, 2012.

[6] V. Hung Nguyen, M. C. Nguyen, H.-V. Nguyen, J. Saint-Martin, and P. Dollfus, "Enhanced thermoelectric figure of merit in vertical graphene junctions," *Applied Physics Letters*, vol. 105, no. 13, Article ID 133105, 2014.

[7] H. Sadeghi, S. Sangtarash, and C. J. Lambert, "Enhancing the thermoelectric figure of merit in engineered graphene nanoribbons," *Beilstein Journal of Nanotechnology*, vol. 6, no. 1, pp. 1176–1182, 2015.

[8] S. R. Akbarabadi, H. Rahimpour Soleimani, and M. Bagheri Tagani, "Side-group-mediated thermoelectric properties of anthracene single-molecule junction with anchoring groups," *Scientific Reports*, vol. 11, no. 8958, pp. 1–18, 2021.

[9] K. S. Novoselov and A. K. Geim, "The rise of graphene," *Nature Materials*, vol. 6, no. 3, pp. 183–191, 2007.

[10] M. M. Asl and B. A. Ravan, "Simulation of infrared absorption properties of single-walled carbon nanotubes," *Journal of Nanoelectronics and Optoelectronics*, vol. 13, no. 1, pp. 27–31, 2018.

[11] L. Tapasztó, G. Dobrik, P. Lambin, and L. P. Biró, "Tailoring the atomic structure of graphene nanoribbons by scanning tunnelling microscope lithography," *Nature Nanotechnology*, vol. 3, no. 7, pp. 397–401, 2008.

[12] K. Wakabayashi, M. Fujita, H. Ajiki, and M. Sigrist, "Electronic and magnetic properties of nanographite ribbons," *Physical Review B*, vol. 59, no. 12, pp. 8271–8282, 1999.

[13] A. H. Castro Neto, F. Guinea, N. M. R. Peres, K. S. Novoselov, and A. K. Geim, "The electronic properties of graphene," *Reviews of Modern Physics*, vol. 81, no. 1, pp. 109–162, 2009.

[14] X. Xu, N. M. Gabor, J. S. Alden, A. M. Van Der Zande, and P. L. McEuen, "Photo-thermoelectric effect at a graphene interface junction," *Nano Letters*, vol. 10, no. 2, pp. 562–566, 2010.

[15] N. Xin, X. Li, C. Jia et al., "Tuning charge transport in aromatic-ring single-molecule junctions via ionic-liquid gating," *Angewandte Chemie*, vol. 130, no. 43, pp. 14222–14227, 2018.

[16] S. Ramezani Akbarabadi, Z. Golsanamlou, and H. Rahimpour Soleimani, "Study of length-dependent tunneling magnetoresistance in two phenyl based molecules," *Current Physical Chemistry*, vol. 4, no. 3, pp. 285–289, 2014.

[17] S. R. Akbarabadi, H. R. Soleimani, M. B. Tagani, and Z. Golsanamlou, "Impact of coupling geometry on thermoelectric properties of oligophenyl-base transistor," *Chinese Physics B*, vol. 26, no. 2, Article ID 027303, 2017.

[18] S. Ramezani Akbarabadi and M. Madadi Asl, "Anchoring groups determine conductance, thermopower and thermoelectric figure of merit of an organic molecular junction," *Frontiers in Physics*, vol. 9, Article ID 727325, 2021.

[19] M. Madadi Asl and S. R. Akbarabadi, "Voltage-dependent plasticity of spin-polarized conductance in phenyl-based single-molecule magnetic tunnel junctions," *PLoS One*, vol. 16, no. 9, Article ID e0257228, 2021.

[20] X. H. Zheng, I. Rungger, Z. Zeng, and S. Sanvito, "Effects induced by single and multiple dopants on the transport properties in zigzag-edged graphene nanoribbons," *Physical Review B*, vol. 80, no. 23, Article ID 235426, 2009.

[21] Y. An, X. Wei, and Z. Yang, "Improving electronic transport of zigzag graphene nanoribbons by ordered doping of b or n atoms," *Physical Chemistry Chemical Physics*, vol. 14, no. 45, pp. 15802–15806, 2012.

[22] G. R. Berdiyorov, H. Bahlouli, and F. M. Peeters, "Effect of substitutional impurities on the electronic transport properties of graphene," *Physica E: Low-Dimensional Systems and Nanostructures*, vol. 84, pp. 22–26, 2016.

[23] D. Wei, Y. Liu, Y. Wang, H. Zhang, L. Huang, and G. Yu, "Synthesis of n-doped graphene by chemical vapor deposition and its electrical properties," *Nano Letters*, vol. 9, no. 5, pp. 1752–1758, 2009.

[24] B. Guo, Q. Liu, E. Chen, H. Zhu, L. Fang, and J. R. Gong, "Controllable n-doping of graphene," *Nano Letters*, vol. 10, no. 12, pp. 4975–4980, 2010.

[25] S. Dutta, A. K. Manna, and S. K. Pati, "Intrinsic half-metallicity in modified graphene nanoribbons," *Physical Review Letters*, vol. 102, no. 9, Article ID 096601, 2009.

[26] B. Biel, X. Blase, F. Triozon, and S. Roche, "Anomalous doping effects on charge transport in graphene nanoribbons," *Physical Review Letters*, vol. 102, no. 9, Article ID 096803, 2009.

[27] Q. Wu, H. Sadeghi, V. M. García-Suárez, J. Ferrer, and C. J. Lambert, "Thermoelectricity in vertical graphene-C60-graphene architectures," *Scientific Reports*, vol. 7, no. 1, pp. 11680–11688, 2017.

[28] N. Al-Aqtash, K. M. Al-Tarawneh, T. Tawalbeh, and I. Vasiliev, "Ab initio study of the interactions between boron and nitrogen dopants in graphene," *Journal of Applied Physics*, vol. 112, no. 3, Article ID 034304, 2012.

[29] Y. Ouyang and J. Guo, "A theoretical study on thermoelectric properties of graphene nanoribbons," *Applied Physics Letters*, vol. 94, no. 26, Article ID 263107, 2009.

[30] Y. Chen, T. Jayasekera, A. Calzolari, K. W. Kim, and M. Buongiorno Nardelli, "Thermoelectric properties of graphene nanoribbons, junctions and superlattices," *Journal of Physics: Condensed Matter*, vol. 22, no. 37, Article ID 372202, 2010.

[31] B. K. Nikolić, K. K. Saha, T. Markussen, and S. T. Kristian, "First-principles quantum transport modeling of thermoelectricity in single-molecule nanojunctions with graphene nanoribbon electrodes," *Journal of Computational Electronics*, vol. 11, no. 1, pp. 78–92, 2012.

[32] D. Sánchez-Portal, P. Ordejon, E. Artacho, and J. M. Soler, "Density-functional method for very large systems with lcao basis sets," *International Journal of Quantum Chemistry*, vol. 65, no. 5, pp. 453–461, 1997.

[33] J. P. Perdew, K. Burke, and M. Ernzerhof, "Generalized gradient approximation made simple," *Physical Review Letters*, vol. 77, no. 18, pp. 3865–3868, 1996.

[34] M. Brandbyge, J.-L. Mozos, P. Ordejón, J. Taylor, and K. Stokbro, "Density-functional method for nonequilibrium electron transport," *Physical Review B*, vol. 65, no. 16, Article ID 165401, 2002.

[35] Y. Meir and N. S. Wingreen, "Landauer formula for the current through an interacting electron region," *Physical Review Letters*, vol. 68, no. 16, pp. 2512–2515, 1992.

[36] S. Datta, *Quantum Transport: Atom to Transistor*, Cambridge University Press, Cambridge, UK, 2005.

[37] L. G. C. Rego and G. Kirczenow, "Quantized thermal conductance of dielectric quantum wires," *Physical Review Letters*, vol. 81, no. 1, pp. 232–235, 1998.

[38] M. Strange, J. S. Seldenthuis, C. J. Verzijl, J. M. Thijssen, and G. C. Solomon, "Interference enhanced thermoelectricity in quinoid type structures," *The Journal of Chemical Physics*, vol. 142, no. 8, Article ID 084703, 2015.

[39] M. Paulsson and S. Datta, "Thermoelectric effect in molecular electronics," *Physical Review B*, vol. 67, no. 24, Article ID 241403, 2003.

[40] C. M. Finch, V. M. Garcia-Suarez, and C. J. Lambert, "Giant thermopower and figure of merit in single-molecule devices," *Physical Review B*, vol. 79, no. 3, Article ID 033405, 2009.

[41] M. Gao, G.-P. Zhang, and Z.-Y. Lu, "Electronic transport of a large scale system studied by renormalized transfer matrix method: application to armchair graphene nanoribbons between quantum wires," *Computer Physics Communications*, vol. 185, no. 3, pp. 856–861, 2014.

[42] H. Dakhlaoui, S. Almansour, W. Belhadj, and B. M. Wong, "Modulating the conductance in graphene nanoribbons with multi-barriers under an applied voltage," *Results in Physics*, vol. 27, Article ID 104505, 2021.